Deformation and Failure of OFHC Copper Under High Strain Rate Shear Compression

Andrew Ruggiero[1,a)], Gabriel Testa[1], Nicola Bonora[1], Gianluca Iannitti[2], Italo Persechino[1] and Magnus Hörnqvist Colliander[3]

[1]*Department of Civil and Mechanical Engineering, University of Cassino and Southern Lazio, Via Di Biasio, 43, Cassino, I-03043 Italy.*
[2]*TECHDYN Engineering, Via Rendano, Rome, I-00199 Italy.*
[3]*Applied Physics, Chalmers University of Technology, Gothenburg, Sweden.*

[a)]Corresponding author: a.ruggiero@unicas.it

Abstract. Hat-shaped specimen geometries were developed to generate high strain, high-strain-rates deformation under prescribed conditions. These geometries offer also the possibility to investigate the occurrence of ductile rupture under low or negative stress triaxiality, where most failure models fail. In this work, three tophat geometries were designed, by means of extensive numerical simulation, to obtain desired stress triaxiality values within the shear region that develops across the ligament. Material failure was simulated using the Continuum Damage Model (CDM) formulation with a unilateral condition for damage accumulation and validated by comparing with quasi-static and high strain rate compression tests results on OFHC copper. Preliminary results seem to indicate that ductile tearing initiates at the specimen corner location where positive stress triaxiality occurs because of local rotation and eventually propagates along the ligament.

INTRODUCTION

In many applications, such as metal forming, crash-worthiness, ballistic impact, etc., shear localization or banding is observed. At high strain rate, thermal softening due to the nearly adiabatic deformation enhances the shear band formation leading to adiabatic shear bands (ASB) [1–3]. This is an important mode of deformation as these shear zones often become the sites for eventual failure of the material.

In most cases the occurrence of adiabatic shearing is undesirable, yet recently developed adiabatic cutting and blanking techniques use this phenomenon to their advantage [4]. For both scenarios the link between localization and ductile damage, in the meaning of nucleation and growth of micro-voids, should be further investigated.

Research on shear banding has typically concentrated on: the modeling of plastic flow instability; and the relationship of shear banding to initial microstructure and its evolution [5]. Some work has been done on damage evolution, where an initial porosity is assumed, and the effect of hydrostatic stress [6]. However, little has been done on damage nucleation or initiation. The scope of this work is to investigate ductile failure initiation in OFHC Cu within the shear region. To this purpose, the forced shear or "tophat" specimen was used [7], because it imposes the position of localization and shear band formation. As an additional advantage, quasistatic and dynamic tests can be performed with the same specimen geometry. Three geometries were designed by finite element analysis in order to obtain different states of the stress triaxiality. Numerical simulations were performed with the implicit finite element code MSC.Marc r2014, in axisymmetric configuration, using four node, isoparametric elements. A coupled thermo-mechanical dynamic transient analysis was performed in order to account for temperature rise due to plastic work. Since the shear region material undergoes large deformation, a global remeshing technique was used to avoid convergence problems and loss of accuracy due to extreme element distortion.

Damage observed in *post mortem* analyses was compared with numerical predictions where material failure was simulated using CDM model formulation. In just one of the three geometries designed, damage occurred. This nucleates in form of a crack at the inner corner between the hat and the brim and, eventually, propagates through the ligament. A tensile state of stress is generated by the large deformation of the structure where damage is observed.

Shock Compression of Condensed Matter - 2015
AIP Conf. Proc. 1793, 100007-1–100007-4; doi: 10.1063/1.4971632
Published by AIP Publishing. 978-0-7354-1457-0/$30.00

MATERIAL

Tests were performed on Oxygen-Free High Conductivity (OFHC) 99.98% copper, obtained in the form of half-hardened bars. After machining of tophat test samples, the material was annealed for 30 minutes at 400°C. The microstructure, analyzed by Electron BackScatter Diffraction (EBSD), manifests a random starting texture. The grain size was estimated to be 14 μm, if the twin boundaries were included, 47 μm if neglected.

From the mechanical point of view, the material was fully characterized at low and high strain rates by means of tensile tests. Both smooth and round notched specimen geometries were used for damage assessment.

CONSTITUTIVE MATERIAL MODEL

The constitutive material model consists of three independent sub-models: a flow stress law, an Equation of State (EoS), and a damage model. The flow stress was modeled with a modified Johnson and Cook law [8], where the first term was replaced by a two-term Voce type law to account for hardening saturation at large strain [9, 10].

$$\sigma = f(\varepsilon)\left(1 + C \ln \frac{\dot{\varepsilon}}{\dot{\varepsilon}_0}\right)(1 - T^{*m}), \tag{1}$$

with,

$$f(\varepsilon) = \sigma_y^0 + B_1\left[1 - \exp\left(-\frac{\varepsilon}{t_1}\right)\right] + B_2\left[1 - \exp\left(-\frac{\varepsilon}{t_2}\right)\right], \tag{2}$$

where ε is the equivalent plastic strain, $\dot{\varepsilon}^* = \dot{\varepsilon}/\dot{\varepsilon}_0$ is the dimensionless plastic strain rate for $\dot{\varepsilon}_0 = 1.0\ \mathrm{s}^{-1}$, and $T^* = (T - T_{room}) / (T_{melt} - T_{room})$ is the homologous temperature. The material constants are σ_y^0, B_1, B_2, t_1, t_2, C, and m.

Regarding the EoS, since the pressure reached in the tophat experiments is rather low, a constant bulk modulus was used to describe the hydrostatic behavior of copper, $K = 130.21$ GPa. The spherical component of the stress tensor is given as $\sigma_H = K\,\Delta V/V$, where $\Delta V/V$ is the volumetric strain.

To model ductile damage nucleation and growth within the shear region, the Bonora's damage model was used [11]. The model was developed in the framework of the CDM, initially proposed by Lemaitre [12]. Under the assumptions of isotropic damage and strain equivalence, the damage variable is related to the effective elastic modulus of the material. Unlike other similar models, damage does not affect the yield function. Damage is a state variable that evolves with the total "active" equivalent plastic strain, ε^+, (i.e. the total equivalent plastic strain accumulated under tensile states of stress). In compression, damage effects are temporarily restored. The kinetic evolution law for the damage variable is given as follow:

$$\mathrm{d}D = \alpha \frac{{D_{cr}}^{\frac{1}{\alpha}}}{\ln\left(\varepsilon_f/\varepsilon_{th}\right)} R_\nu \left(D_{cr} - D\right)^{\frac{\alpha-1}{\alpha}} \frac{\mathrm{d}\varepsilon^+}{\varepsilon^+}, \tag{3}$$

with,

$$R_\nu = \frac{2}{3}(1 - \nu) + 3(1 - 2\nu)\left(\frac{\sigma_H}{\sigma_{eq}}\right)^2. \tag{4}$$

where ν is the Poisson's ratio and σ_{eq} is the von Mises stress.

The model, which results in a non linear damage accumulation with active plastic strain, requires the knowledge of four damage parameters, all having a physical meaning: the damage threshold strain, ε_{th}, at which damage processes initiates; the theoretical failure strain under constant uniaxial state of stress conditions, ε_f, at which ductile failure would occur; the critical damage, D_{cr}, at which failure occurs; and the damage exponent, α, that controls the shape of damage evolution with plastic strain. The parameters can be easily identified with uniaxial tensile tests on smooth and round notched specimen geometries [13, 14]. The values for the annealed OFHC 99.98% Cu are given in Table 1.

Because damage accumulates with plastic strain, in order to obtain a reliable damage prediction, its very important to provide the appropriate strain at the material point.

The strength model used does not account for the effects observed during shear band nucleation and evolution, such as dynamic recrystallization or the breakdown of elongated cells [15]. Since few, if any strength models can capture this physics, the strength model parameters were calibrated for each test configuration to obtain the correct load vs. displacement curves.

TABLE 1. Damage model parameters for OFHC 99.98% Cu.

ε_{th}	ε_f	D_{cr}	α
0.325	2.85	0.15	1.0

RESULTS AND DISCUSSION

To investigate the effect of the stress triaxiality on damage initiation, three different geometries were designed by FE analyses. The parameter that most affects the state of stress in the shear zone of a tophat specimen was found to be the ratio between the inner hole diameter of the brim and the outer hat diameter (ϕ_{in}/ϕ_{out}). However, the parametric analysis performed changing this ratio showed that the states of stress reachable in a hat-shaped specimen are rather limited. A pure shear condition cannot be obtained and, usually, the stress triaxiality factor ($TF = \sigma_H/\sigma_{eq}$), even when uniform within the shear region, is not constant with plastic strain evolution. In Fig. 1(a), a sketch of the hat-specimen geometry is given. Three different inner diameters were used: 5.5 mm for "A"; 6.0 mm for "C", and 6.5 mm for "D". The corresponding stress triaxiality paths calculated simulating the dynamic tests are given in Fig. 1(b), for a generic point within the shear region. Very similar results were obtained for quasi static tests. In tophat "A", the state of stress is always compressive and the TF is rather constant. For the other geometries, the TF increases almost linearly with plastic strain and, starting from a compressive state of stress, this becomes tensile for a plastic strain of 1.7 and 1.2, for the tophats "C" and "D" respectively.

In Fig. 1(c), the section of a tophat (geometry "A") tested under quasistatic loading conditions is shown. No shear banding is evident, instead a diffuse area of shear localization is present. The same was observed for all the geometries, both in quasistatic and dynamic strain regimes.

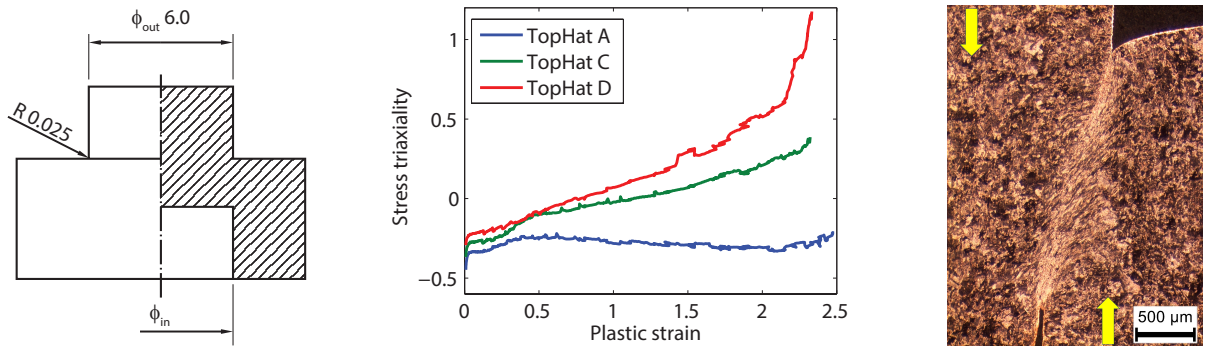

(a) (b) (c)

FIGURE 1. (a) Geometry of tophat specimens (dimensions in mm); (b) Stress triaxiality paths for quasistatic tests; (c) Micrography of the shear deformed region for the quasistatic test on geometry "A" (yellow arrows show the direction of the displacement).

For all tests, a total displacement of approximately 2.7 mm was imposed. For geometries "A" and "C" no voids or cracks were found, whereas for "D" the ligament failed and the upper hat stuck into the brim hole. For "A" and "C", as expected, the load–displacement curves are monotonically increasing, Fig. 2(a). Instead, an instability is present in the curves of the geometry "D", due to damage nucleation and growth and not to shear banding. To confirm this hypothesis, a test stopped just after the instability was performed, tophat "D4", whose micrography confirms the presence of some ductile tearing and a crack propagating from the inner corner of the specimen, Fig. 2(b).

With the experimental load–displacement curves, in Fig. 2(a), the numerical curves, calculated after calibration of the strength model parameters, are given for comparison. The load drop obtained simulating the tests on geometry ''D" is due to crack generation and propagation. From a numerical point of view, this is fulfilled with the element removal technique that is used once the value of critical damage is reached. Damage predictions are in good agreement with experimental evidence. For the final displacement of the test "D4" (1.9 mm), some damage accumulates at the external corner region without reaching the critical value. Instead, at the inner corner, critical damage is reached in some elements leading to the crack generation and propagation, Fig. 2(c).

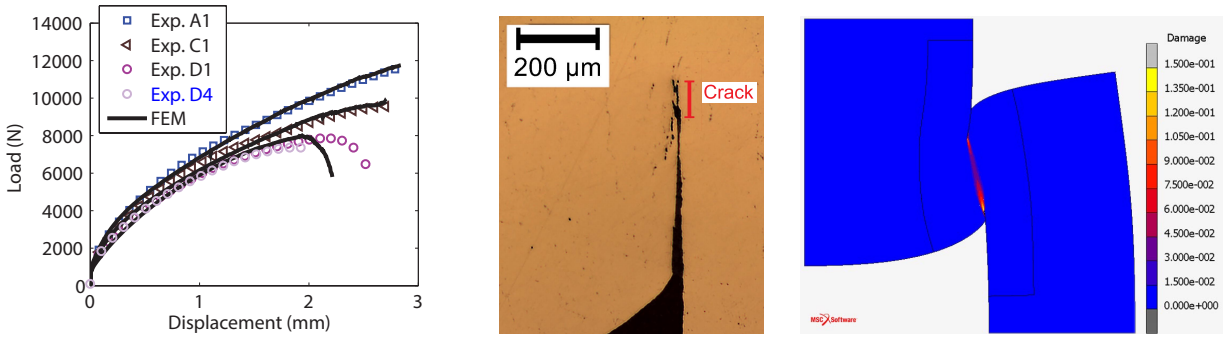

(a) (b) (c)

FIGURE 2. (a) Load–displacement curves for quasistatic tests; (b) Micrography of the internal corner regions for tophat "D4"; (c) Map of calculated damage for tophat "D4" (D_{cr} = 0.15).

CONCLUSIONS

The tophat specimen was used to investigate damage initiation in the shear localization regions under quasi static and dynamic loading. Different geometries were adopted to generate different regimes of stress triaxiality. For each configuration, strength model parameters were calibrated to obtain the correct load-displacement curve. Once calibrated, FE models provide prediction of damage nucleation and evolution in good agreement with experimental data. Results demonstrate that, at least for Cu, damage occurs only under positive stress triaxiality conditions, consistent with the assumption in the damage model.

REFERENCES

[1] R. J. Clifton, J. Duffy, K. A. Hartley, and T. G. Shawki, Scripta Metallurgica **18**, 443–448 (1984).
[2] C. Zener and J. H. Hollomon, Journal of Applied Physics **15**, 22–32 (1944).
[3] D. Rittel, Z. G. Wang, and M. Merzer, Physical Review Letters **96**, p. 075502 (2006).
[4] J. Peirs, P. Verleysen, J. Degrieck, and F. Coghe, International Journal of Impact Engineering **37**, 703–714 (2010).
[5] E. Cerreta, J. Bingert, C. Trujillo, M. Lopez, C. Bronkhorst, B. Hansen, and G. Gray, "Dynamic shear deformation in high purity iron," in *DYMAT 2009 - 9th International Conference on the Mechanical and Physical Behaviour of Materials under Dynamic Loading*, Vol. 2 (2009), pp. 977–983.
[6] C. A. Bronkhorst, E. K. Cerreta, Q. Xue, P. J. Maudlin, T. A. Mason, and G. T. Gray III, International Journal of Plasticity **22**, 1304–1335 (2006).
[7] K.-H. Hartmann, H.-D. Kunze, and L. Meyer, "Metallurgical effects on impact loaded materials," in *Shock waves and high-strain-rate phenomena in metals*, edited by M. A. Meyers and L. Murr (Springer, 1981), pp. 325–337.
[8] G. R. Johnson and W. H. Cook, "A constitutive model and data for metals subjected to large strains, high strain rates and high temperatures," in *7th International Symposium on Ballistics* (1983), pp. 541–547.
[9] M. Hörnqvist, N. Mortazavi, M. Halvarsson, A. Ruggiero, G. Iannitti, and N. Bonora, Acta Materialia **89**, 163–180 (2015).
[10] N. Bonora, G. Testa, A. Ruggiero, G. Iannitti, N. Mortazavi, and M. Hörnqvist, Journal of Dynamic Behavior of Materials **1**, 136–152 (2015).
[11] N. Bonora, Engineering Fracture Mechanics **58**, 11–28 (1997).
[12] J. Lemaitre, Journal of Engineering Material and Technology **107**, 83–89 (1985).
[13] N. Bonora, A. Ruggiero, L. Esposito, and D. Gentile, International Journal of Plasticity **22**, 2015–2047 (2006).
[14] N. Bonora, A. Ruggiero, D. Gentile, and S. De Meo, Strain **47**, 241–254 (2011).
[15] M. Meyers, U. Andrade, and A. Chokshi, Metallurgical and Materials Transactions A **26**, 2881–2893 (1995).